

# Effect of surface roughness on nonlinear reflection of weak shock waves

Maria M. Karzova,<sup>1,a)</sup> Thomas Lechat,<sup>2</sup> Sébastien Ollivier,<sup>3</sup>  
Didier Dragna,<sup>2</sup> Petr V. Yuldashev,<sup>1</sup> Vera A. Khokhlova,<sup>1</sup>  
and Philippe Blanc-Benon<sup>2</sup>

<sup>1</sup>Faculty of Physics, M. V. Lomonosov Moscow State University, Moscow 119991, Russia

<sup>2</sup>Université de Lyon, Ecole Centrale de Lyon, Institut National des Sciences Appliquées de Lyon, Université Claude Bernard Lyon I, Centre National de la Recherche Scientifique, Laboratoire de Mécanique des Fluides et d'Acoustique, Unité Mixte de Recherche 5509, 36 Avenue Guy de Collongue, F-69134, Ecully, France

<sup>3</sup>Université de Lyon, Université Claude Bernard Lyon I, Ecole Centrale de Lyon, Institut National des Sciences Appliquées de Lyon, Centre National de la Recherche Scientifique, Laboratoire de Mécanique des Fluides et d'Acoustique, Unité Mixte de Recherche 5509, 43 Boulevard du 11 Novembre 1918, F-69100, Villeurbanne, France

masha@acs366.phys.msu.ru, thomas.lechat@ec-lyon.fr, sebastien.ollivier@ec-lyon.fr,  
didier.dragna@ec-lyon.fr, petr@acs366.phys.msu.ru, vera@acs366.phys.msu.ru,  
philippe.blanc-benon@ec-lyon.fr

**Abstract:** The authors have recently shown that irregular reflections of spark-generated pressure weak shocks from a smooth rigid surface can be studied using an optical interferometer [Karzova, Lechat, Ollivier, Dragna, Yuldashev, Khokhlova, and Blanc-Benon, *J. Acoust. Soc. Am.* **145**(1), 26–35 (2019)]. The current study extends these results to the reflection from rough surfaces. A Mach-Zehnder interferometer is used to measure pressure waveforms. Simulations are based on the solution of axisymmetric Euler equations. It is shown that roughness causes a decrease of the Mach stem height and the appearance of oscillations in the pressure waveforms. Close to rough surfaces, the pressure was higher compared to the smooth surface.

© 2019 Acoustical Society of America

[TDM]

Date Received: July 18, 2019 Date Accepted: October 11, 2019

## 1. Introduction

Irregular reflection is a classical phenomenon of shock wave physics discovered experimentally by Ernst Mach and then theoretically studied by John von Neumann.<sup>1,2</sup> Irregular reflection can be broadly classified into two types, namely, Mach reflection and von Neumann reflection.<sup>3</sup> Mach reflection is typical for strong shocks (Mach number  $>1.47$ ) and comprises at least three shocks in the reflection pattern: incident and reflected shocks intersected above the surface, and a Mach stem that links this intersection point with the surface. In Mach reflection, the intersection point is a point of discontinuity and is called a triple point. The von Neumann reflection concerns weak acoustic shocks (Mach number  $<1.47$ ) and differs from the Mach reflection by the absence of slope discontinuity between the reflected shock and the Mach stem.<sup>4</sup> In this case the Mach stem refers to the single shock that forms between the surface and the point where the incident shock and the reflected shock start to separate.

Nonlinear reflections of weak acoustic shock waves, though irregular, cannot be described by the three-shock theory of von Neumann<sup>3</sup> according to the von Neumann paradox. Experimental observation of irregular reflection of weak shock acoustic waves is challenging because of different features. First of all, in laboratory-scales weak acoustic shock waves have a very small shock thickness (less than 0.1 mm) and a very short rise time ( $<1 \mu\text{s}$ ). In air it is then impossible to measure pressure waveforms in irregular reflection patterns using classical methods based on microphones. Only very few experiments showed weak acoustic shockwave irregular reflection patterns and the evolution of the Mach stem with the distance from the source. In case of a flat smooth reflecting surface, the evolution of the Mach stem and pressure waveforms were measured in a moderate-scale outdoor experiment in air for gaseous

<sup>a)</sup>Author to whom correspondence should be addressed. Also at: Université de Lyon, Ecole Centrale de Lyon, INSA Lyon, Université Claude Bernard Lyon I, CNRS, LMFA, UMR 5509, 36 Avenue Guy de Collongue, F-69134, Ecully, France.

explosions,<sup>5</sup> in a laboratory scale experiment in water for ultrasound sawtooth waves,<sup>6</sup> and in laboratory-scale experiments in air for spark-generated waves.<sup>7–9</sup>

The geometry of the reflective surface is one of the factors that strongly affects the reflection patterns. For example, a recent numerical study of reflection of ideal weak *N*-wave from a convex-concave boundary showed a complex five-shock pattern in irregular reflection.<sup>10</sup> Another important factor is surface roughness. The effect of roughness on the evolution of the Mach stem and on reflection patterns has been addressed for high amplitude and moderate shocks.<sup>11–13</sup> However to our knowledge, it has never been investigated and observed for weak acoustic shock waves.

The goal of the present letter is to show how the presence of roughness on a plane surface changes pressure waveforms and affects on the Mach stem formation compared to the reference case of a perfectly rigid and flat surface. In our recent study<sup>9</sup> the optical Mach-Zehnder interferometer method was proposed to reconstruct pressure waveforms in case of irregular reflection patterns for spherically diverging spark-generated shock pulses from a plane smooth rigid surface in air. Irregular reflection patterns obtained by numerical simulations of axisymmetric Euler equations were in good agreement with experimental ones. Here, we present results obtained for rough surfaces with the same experimental and numerical methods as described in Ref. 9.

## 2. Methods

### 2.1 Experiment

Recently, it was shown that the Mach-Zehnder optical interferometry method allows to reconstruct acoustic pressure waveforms both in free field<sup>14</sup> and close to a reflecting boundary.<sup>9</sup> This method has a time resolution of 0.4  $\mu$ s, which is more than 6 times higher than the time resolution of standard condenser microphones like B&K (Brüel & Kjær, Denmark), type 4138 (2.9  $\mu$ s). Moreover, it allows quantitative reconstruction of the pressure waveform directly in Pascals without the need of additional calibration and could be applied in situations where microphones distort the acoustic field. The main limitation of the method is that the wavefront geometry must be spherical or cylindrical to allow the application of the inverse Abel transform in the signal processing. The method has been detailed in Ref. 14 and its implementation in the case of shock wave reflection from the plane surface is presented in Ref. 9. Here, we only briefly describe the acoustical part of the experimental setup and the measurement protocol.

The sound source is an electrical spark positioned at a height of  $z_s = 21$  mm above a surface [Fig. 1(a)]. The spark source is made of two tungsten electrodes separated by a gap of 20 mm and supplied by an electrical voltage in the range of 15–20 kV. The spark generates spherically divergent pressure waves that are similar to *N*-waves or blast waves. The spark-generated shock pulse has a pressure amplitude of about 0.8 kPa, a duration of about 50  $\mu$ s, and a shock width of 100  $\mu$ m at 30 cm from the source.<sup>15</sup>

Three surfaces were used as reflective boundaries: a plane rigid surface made of PVC as a reference surface<sup>9</sup> and two rough surfaces obtained by gluing sheets of standard sandpapers called “P80” and “P40” on the PVC board. The height  $\sigma$  of the rough surfaces P80 and P40 was characterized using a digital microscope VHX-6000 (Keyence, USA) [Fig. 1(b)]. The analysis of the roughness leads to isotropic correlated Gaussian distributions with standard deviation of the surface height equal to 66 and 129  $\mu$ m for P80 and P40, respectively. The correlation length is 181 and 337  $\mu$ m for P80 and P40, respectively. Note that these characteristic lengths of the roughness are smaller or on the order of the shock width.<sup>15</sup>

To measure the pressure waveform, a probe laser beam of the interferometer was positioned at different heights  $z$  above the surface from 2 up to 25 mm and at a horizontal distance  $r = 33$  cm. For the chosen geometry the angle of incidence was 3.4°, and the Mach number was equal to 1.005. In experiments, 140 waveforms were recorded at

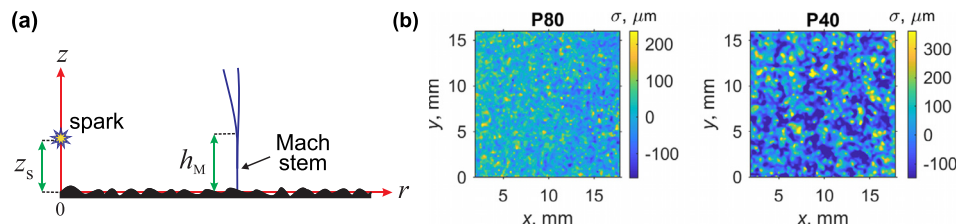


Fig. 1. (Color online) (a) Scheme illustrating the reflection of a spark-generated pulse from a rough surface. (b) Surface texture of P80 and P40 sandpapers measured using a digital microscope VHX-6000.

each height  $z$  in order to allow statistical data analysis. A representative waveform was selected among these 140 with values of arrival time, peak positive pressure, and peak negative pressure closest to average values computed over all waveforms.

## 2.2 Numerical model

The numerical model is based on axisymmetric Euler equations and is described in detail in Ref. 9. Simulations were performed using a high order finite-difference time-domain algorithm. In order to study the reflection over rough surfaces, a curvilinear coordinate system that fits the surface shape is applied.<sup>16</sup>

Transition from Cartesian coordinates  $(r, z)$  to the curvilinear coordinate system  $(\zeta, \eta)$  requires reformulation of partial derivatives in the Euler equations. Cartesian coordinates are expressed as functions of curvilinear ones,

$$r = \zeta, \quad (1)$$

$$z = \eta \left( \frac{z_m - \sigma(\zeta)}{z_m} \right) + \sigma(\zeta), \quad (2)$$

where  $\sigma(\zeta)$  corresponds to the surface height and  $z_m$  is the maximum elevation of the simulation window.

There is no deformation of the mesh at the top of the domain while the deformation of the mesh is maximal at the surface. All partial spatial derivatives are then expressed in this new coordinate system. The surface is assumed to be perfectly reflecting. The normal velocity at the surface is then set to zero. Particular attention is paid to the expression of this boundary condition in the curvilinear coordinate system.

Based on the surface measurements the surface height is modeled as a correlated Gaussian distribution. The standard deviation of the height and the correlation length are set with the values obtained experimentally (Sec. 2.1). Since the numerical solver is axisymmetric, the surface geometry is also axisymmetric, the axis of symmetry being perpendicular to the surface which contains the source. The spark source is modeled as an instantaneous energy injection with a Gaussian shape, as described in Ref. 9.

## 3. Results

Waveforms measured at 2 and 16 mm above the surface and at a horizontal distance of  $r = 33$  cm are shown in Fig. 2. Three cases are presented: the smooth surface, P80, and P40 sandpapers. Above the smooth surface, both at 2 and 16 mm, only a single front shock is present. This shock corresponds to the Mach stem. The pressure rise is very steep and is related to the rise time of the measurement method. Above the P80 rough surface, at 2 mm height, the front shock has two slopes, the positive peak pressure is 15% higher than for the smooth case and oscillations appear after the peak, with a characteristic time on the order of 6  $\mu$ s. At 16 mm above the P80, the positive peak is rounded, its amplitude is lower than for the smooth case, and the pressure rise consists of two separated shocks. Thus, in the case of P80 the first measurement at 2 mm corresponds to the Mach stem since there is a single shock front, while at 16 mm the measurement is above the Mach stem as separation between the incident and reflected shocks is clearly observed. Above the P40 surface, at 2 mm the incident and reflected shocks can be seen. Thus no Mach stem is formed or it is smaller than 2 mm. The positive peak is more rounded. The two shocks are more clearly seen on the waveform measured at 16 mm. Oscillations also appear in the waveform after the peak, but with a longer characteristic time than for P80. These observations highlight the influence of roughness on the waveforms: with roughness the Mach stem is shorter than for reflections from a smooth surface, and if the roughness is too large there is no Mach

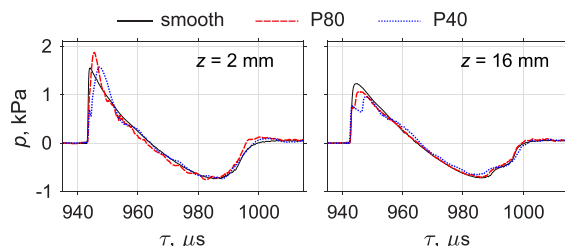


Fig. 2. (Color online) Waveforms measured using the Mach-Zehnder interferometer at  $r = 33$  cm for smooth surface (solid curves), rough surface P80 (dashed curves), and P40 (dotted curves) at heights of 2 mm (left) and 16 mm (right).

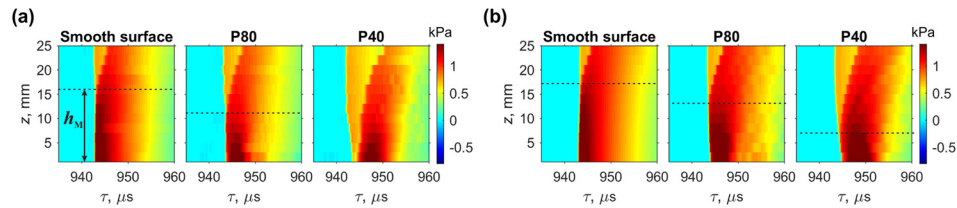


Fig. 3. (Color online) (a) Reflection patterns measured using the Mach-Zehnder interferometer at  $r = 33$  cm for the smooth surface and rough surfaces P80 and P40. (b) Numerically simulated reflection patterns obtained for the cases shown in (a).

stem. Oscillations appear in the waveform, and their characteristic time is related to the roughness size. Note that such observation is only possible thanks to the very high temporal and spatial resolution of the optical interferometer, and such details could not be observed using microphones, any usual pressure sensors, or Schlieren images.

To obtain reflection patterns in the spatio-temporal domain, waveforms are measured at different heights above the surface, then the pressure amplitude is converted into color, and the resulting horizontal color bar is plotted at the corresponding height. Results given in Fig. 3(a) show the reflection patterns obtained from the measured waveforms at  $r = 33$  cm from the source. These reconstructed reflection patterns show that the roughness decreases the length of the Mach stem: for the smooth surface the Mach stem height is 16 mm, for P80 it is 12 mm, and for the biggest roughness, P40, there is no Mach stem at all.

In order to confirm these observations, numerical simulations were performed with parameters corresponding to the experiment (same free field level, same statistical parameters for the rough surface). For comparison, reflection patterns are plotted in the same way as for the experiments in Fig. 3(b). Simulated reflection patterns are in good agreement with the experimental ones, but with slightly higher Mach stems. This small overestimation was also observed in the analysis of the reflection over a smooth surface. Since the numerical model assumes a two-dimensional axisymmetric geometry, a perfectly rigid surface, and it is based on a model for the spark source, some differences between simulations and measurements are expected. The difference in the negative part of measured and simulated pressure waveforms (Fig. 4) comes from the source initialization in the numerical model.<sup>9</sup> However, the positive part of the waveform is well reproduced, and the same effect is found in numerical simulations: the Mach stem height decreases with increasing roughness size [Fig. 3(b)]. In simulations, a short Mach stem still exists for the P40 surface, but further simulations for slightly larger roughness (not shown here) also confirm that when the roughness is too large, the Mach stem no longer exists. One should also note the change in shape of the shock close to the surface, which seems to be delayed by the roughness.

In order to analyze the effects on the waveforms in more detail, waveforms measured and simulated at different heights above the surface are plotted in Fig. 4 for the same distance ( $r = 33$  cm). Simulated waveforms are very similar to the experimental ones. Oscillations induced by roughness also appear in simulated waveforms, and their amplitude is higher than for experimental ones. Possible reasons for this could be better resolution in time and space, better signal-to-noise ratio in simulations, and also

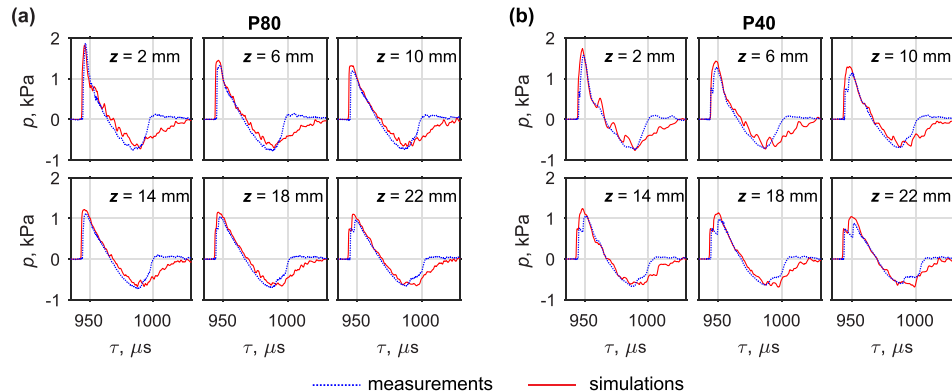


Fig. 4. (Color online) (a) Comparison of measured (dotted curves) and simulated (solid curves) waveforms obtained for P80 (a) and P40 (b) rough surfaces at a horizontal distance  $r = 33$  cm and different heights  $z$  above the surfaces.

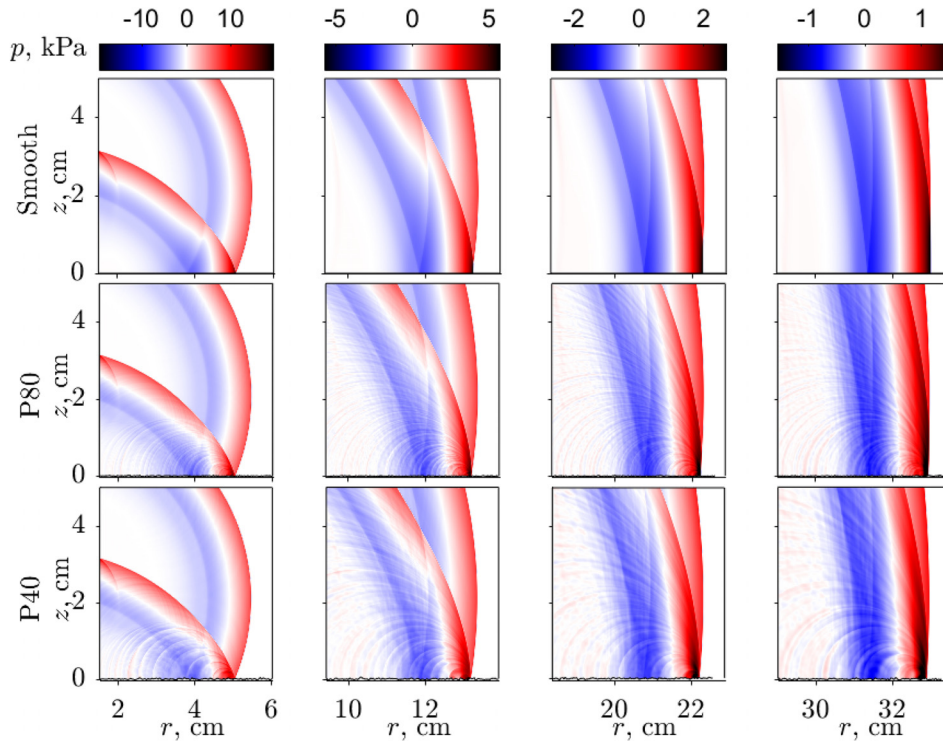


Fig. 5. (Color online) Frames from [Mm. 1](#) showing the spatial evolution of the pressure reflection patterns with the distance for the smooth surface and rough surfaces P80 and P40.

higher coherence of the diffracted field due to the axial symmetry of the numerical model. As observed experimentally, the characteristic time of the oscillations depends on the size of the roughness grain and it is longer for larger grains. The amplitude of oscillations is also higher close to the surface.

To highlight the correlation between the oscillations in the waveforms and the roughness geometry, [Mm. 1](#) has been composed from numerical simulations. It shows the spatial evolution of the pressure reflection patterns with the distance in a moving observation window, starting just after the spark discharge. Three representative cases are shown: the smooth surface for reference, P80, and P40 rough surfaces. A sequence of backscattered waves is clearly seen (see Fig. 5). The backscattered field distorts the rear part of the wave, which corresponds to the oscillations seen previously in the time domain waveforms (Fig. 4). The distance between the backscattered waves depends on the distance between the biggest grains. It is longer for the P40 case than for P80. The amplitude of the backscattered waves is related to the roughness height.

[Mm. 1](#). Spatial evolution of the pressure reflection patterns with the distance for the smooth surface and rough surfaces P80 and P40. This is a file of type “mp4” (6 Mb).

One should also note that in [Mm. 1](#), the area where the overpressure is the highest is just behind the front shock and close to the surface. Also note that the pressure amplitudes close to surfaces P80 and P40 are higher than those observed in the case of the smooth surface.

The pressure levels in simulations can be analyzed closer to the surface than in experiments. A statistical analysis over 20 numerical realizations for each rough surface (P40 and P80) shows that at  $r = 33$  cm and  $z = 1$  mm the mean value of the pressure amplitude is 1.95 kPa (standard deviation 3.3%) for P80 and 1.86 kPa (standard deviation 5.4%) for P40 (not shown here). Compared to the smooth surface case (1.55 kPa), these values are 26% and 20% higher for P80 and P40, respectively. Thus, we can also conclude that the roughness leads to the increase of the pressure amplitude near the surface for the considered roughness size.

#### 4. Conclusion

A preliminary analysis of the influence of the roughness on the reflection of weak acoustic shock waves was conducted using both optical measurements and numerical simulations. The Mach-Zehnder interferometry method was used to reconstruct pressure waveforms to show irregular reflection patterns. Axisymmetric Euler equations combined with a rough rigid boundary with Gaussian distribution were used in

simulations. Both experimental and numerical results showed that the height of the Mach stem decreases with the growth of the surface grain, and no longer appears when the roughness is sufficiently large. The waveforms close to the surface are distorted by the roughness, the oscillations are related to the grain size, and their amplitude is higher close to the surface. Moreover, the positive peak pressure level close to the rough surface could be higher than in the case of the smooth surface.

In order to further investigate how waveform distortion and Mach stem height are related to roughness parameters, a numerical study of the reflection of weak shocks from surfaces with roughness of different shapes and different scales will be led in the future. In linear acoustics, models based on effective impedance boundary conditions are used to simulate some of the roughness effects. Their applicability to weak shock waves will also be studied.

### Acknowledgments

This work is supported by RSF-17-72-10277 and by the Labex CeLyA of Université de Lyon, operated by the French National Research Agency (ANR-10-LABX-0060/ANR-16-IDEX-0005). The numerical study was conducted within the framework of LETMA (Laboratoire ETudes et Modélisation Acoustique), a Contractual Research Laboratory shared between CEA, CNRS, Ecole Centrale de Lyon, C-Innov, and Sorbonne Université. It was granted access to the HPC resources of IDRIS under the allocation A0042A02203 made by GENCI. The authors are grateful to Thomas Malhomme (research engineer, Laboratoire de Tribologie et Dynamique des Systèmes, UMR CNRS 5513) for performing microscope measurements of sandpapers.

### References and links

- <sup>1</sup>P. Krehl and M. van der Geest, "The discovery of the Mach reflection effect and its demonstration in an auditorium," *Shock Waves* **1**(1), 3–15 (1991).
- <sup>2</sup>J. von Neumann, "Oblique reflection of shocks," in *John von Neumann Collected Work*, edited by A. H. Taub (MacMillan, New York, 1963), Vol. 6, pp. 238–299.
- <sup>3</sup>G. Ben-Dor, *Shock Wave and High Pressure Phenomena* (Springer, New York, 2007), Vol. 2.
- <sup>4</sup>S. Baskar, F. Coulouvrat, and R. Marchiano, "Nonlinear reflection of grazing acoustic shock waves: Unsteady transition from von Neumann to Mach to Snell-Descartes reflections," *J. Fluid. Mech.* **575**, 27–55 (2007).
- <sup>5</sup>K. M. Leete, K. L. Gee, and T. B. Nielsen, "Mach stem formation in outdoor measurements of acoustic shocks," *J. Acoust. Soc. Am.* **138**(6), EL522–EL527 (2015).
- <sup>6</sup>R. Marchiano, S. Baskar, F. Coulouvrat, and J.-L. Thomas, "Experimental evidence of deviation from mirror reflection for acoustical shock waves," *Phys. Rev. E* **76**, 056602 (2007).
- <sup>7</sup>M. Karzova, V. Khokhlova, E. Salze, S. Ollivier, and P. Blanc-Benon, "Mach stem formation in reflection and focusing of weak shock acoustic pulses," *J. Acoust. Soc. Am.* **137**(6), EL436–EL442 (2015).
- <sup>8</sup>C. Desjouy, S. Ollivier, O. Marsden, M. Karzova, and P. Blanc-Benon, "Irregular reflection of weak acoustic shock pulses on rigid boundaries: Schlieren experiments and direct numerical simulation based on a Navier-Stokes solver," *Phys. Fluids* **28**, 027102 (2016).
- <sup>9</sup>M. Karzova, T. Lechat, S. Ollivier, D. Dragna, P. Yuldashev, V. Khokhlova, and P. Blanc-Benon, "Irregular reflection of spark-generated shock pulses from a rigid surface: Mach-Zehnder interferometry measurements in air," *J. Acoust. Soc. Am.* **145**(1), 26–35 (2019).
- <sup>10</sup>B. Tripathi, S. Baskar, F. Coulouvrat, and R. Marchiano, "Numerical observation of secondary Mach stem in weak acoustic shock reflection," *J. Acoust. Soc. Am.* **144**(2), EL125–EL130 (2018).
- <sup>11</sup>T. Suzuki, T. Adachi, and S. Kobayashi, "Experimental analysis of reflected shock behavior over a wedge with surface roughness," *JSME Int. J. Ser. B* **36**(1), 130–134 (1993).
- <sup>12</sup>B. Skews, "Oblique reflection of shock waves from rigid porous materials," *Shock Waves* **4**, 145–154 (1994).
- <sup>13</sup>P. Huber and D. McFarland, "Effect of surface roughness on characteristics of spherical shock waves," *NASA TR R-23*, 1–46 (1955).
- <sup>14</sup>P. Yuldashev, M. Karzova, V. Khokhlova, S. Ollivier, and P. Blanc-Benon, "Mach-Zehnder interferometry method for acoustic shock wave measurements in air and broadband calibration of microphones," *J. Acoust. Soc. Am.* **137**(6), 3314–3324 (2015).
- <sup>15</sup>P. Yuldashev, S. Ollivier, M. Averianov, O. Sapozhnikov, V. Khokhlova, and P. Blanc-Benon, "Nonlinear propagation of spark-generated *N*-waves in air: Modeling and measurements using acoustical and optical methods," *J. Acoust. Soc. Am.* **128**(6), 3321–3333 (2010).
- <sup>16</sup>D. Dragna, P. Blanc-Benon, and F. Poisson, "Time-domain solver in curvilinear coordinates for outdoor sound propagation over complex terrain," *J. Acoust. Soc. Am.* **133**(6), 3751–3763 (2013).